

A precision calculation of relic neutrino decoupling

Kensuke Akita^{1*} and Masahide Yamaguchi^{1†}

¹*Department of Physics, Tokyo Institute of Technology, Tokyo 152-8551, Japan*

Abstract

We study the distortions of equilibrium spectra of relic neutrinos due to the interactions with electrons, positrons, and neutrinos in the early Universe. We solve the integro-differential kinetic equations for the neutrino density matrix, including three-flavor oscillations and finite temperature corrections from QED up to the next-to-leading order $\mathcal{O}(e^3)$ for the first time. In addition, the equivalent kinetic equations in the mass basis of neutrinos are directly solved, and we numerically evaluate the distortions of the neutrino spectra in the mass basis as well, which can be easily extrapolated into those for non-relativistic neutrinos in the current Universe. In both bases, we find the same value of the effective number of neutrinos, $N_{\text{eff}} = 3.044$, which parameterizes the total neutrino energy density.

*E-mail address: kensuke@th.phys.titech.ac.jp

†E-mail address: gucci@phys.titech.ac.jp

Contents

1	Introduction	3
2	Neutrino decoupling	4
2.1	Boltzmann equations in the flavor basis	4
2.2	Boltzmann equations in the mass basis	9
2.3	Finite temperature corrections from QED	12
2.4	Computational method and initial conditions	14
3	Results	15
3.1	The flavor basis	15
3.2	The mass basis	19
3.3	Transformation of distributions in the flavor and mass bases	21
4	Conclusions	21
A	Kinetic equations for neutrinos in comoving variables	22
B	Analytic estimation of the collision integral	25

1 Introduction

The successful hot big bang model after inflation predicts that neutrinos produced in the early Universe still exist in the current Universe. These relic neutrinos are confirmed indirectly by the observations of primordial abundances of light elements from Big Bang Nucleosynthesis (BBN), the anisotropies of the Cosmic Microwave Background (CMB) and the distribution of Large Scale Structure (LSS) of the Universe.

The cosmic neutrino background was generated at high temperature and kept in thermal equilibrium through weak interactions. When the temperature of the Universe decreased, weak interactions became ineffective and cosmic neutrinos were decoupled with other particles at the decoupling temperature $T_{\text{dec}} \sim 2$ MeV. In the instantaneous decoupling limit, the energy spectrum of neutrinos approximately takes a form of Fermi-Dirac distribution function and receives only the effect of redshift of physical momentum after the decoupling. Soon after the decoupling of neutrinos, electrons and positrons start to annihilate and to heat photons when the temperature of the Universe is almost equal to the electron mass $m_e = 0.511$ MeV. If we assume that electrons and positrons annihilate only into photons, we can approximately estimate the ratio of the temperatures of cosmic photons and neutrinos, $T_\gamma/T_\nu \simeq 1.40102$, using the entropy conservation of the Universe.

However, the decoupling temperature of neutrinos T_{dec} and the temperature of annihilation of electrons and positrons are so close that some neutrinos keep interacting with electrons and positrons. These interaction processes become more efficient for neutrinos with higher energies because the interaction rates of relativistic particles with higher energies are larger [1, 2]. Due to these processes, non-thermal distortions in the neutrino spectra are produced and the photon temperature increases less than that in the instantaneous decoupling limit. In particular, the non-thermal distortions increase the total energy density of neutrinos, which can be parameterized by the effective number of neutrinos N_{eff} . This parameter can be constrained by cosmological observations such as the measurement of the CMB anisotropies.

The non-instantaneous decoupling of neutrinos was studied numerically for a long time. In particular, this numerical study requires solving integro-differential kinetic equations, which correspond to the Boltzmann equations for neutrino momentum distributions. First, several studies [3–5] solved these Boltzmann equations under some approximations such as Maxwell-Boltzmann statistics approximation for neutrinos. A few years later, the Boltzmann equations for the distorted Fermi-Dirac statistics of neutrinos were solved in refs. [6–9]. Finally, the kinetic equations were solved with including finite temperature radiative corrections at leading order [10–15] and three-flavor neutrino oscillations [16–18]. The kinetic equations including neutrino oscillations correspond to the Boltzmann equations for the neutrino density matrix. In refs. [16, 18], the authors solved the Boltzmann equations under the damping approximation, where the off-diagonal parts of the collision terms are treated as the damping factors. In ref. [17], the Boltzmann equations for the neutrino density matrix with the full collision terms were solved.

In the present Universe, since the average magnitude of momenta for neutrinos is $\langle p \rangle \sim 0.53$ meV $\ll \sqrt{\Delta m_{21}^2}, \sqrt{|\Delta m_{31}^2|}$, two massive neutrinos at least are non-relativistic. In the non-relativistic epoch for neutrinos, we cannot quantize flavor neutrinos, which are

flavor eigenstates of neutrinos, in the conventional way as we quantize fields whose masses are diagonalized, and hence the flavor neutrino spectra in this epoch do not make sense. In order to investigate and to detect the neutrino spectra in the present epoch, we need to consider massive neutrino spectra. Then, in this paper, by solving the kinetic equations for massive neutrinos in the early Universe, we study the distortions for neutrino spectra in the mass basis too, which could be easily extrapolated to those in the current epoch, and compare the results both in the flavor and mass bases. In addition, since we can expect the better accuracy on future measurements of N_{eff} , we solve the Boltzmann equations for the neutrino density matrix with full collision terms, including finite temperature corrections from QED up to the next-to-leading order $\mathcal{O}(e^3)$ for the first time.

This paper is organized as follows. In Sec. 2, we give the Boltzmann equations both in the flavor and mass bases in order to analyze the decoupling process of neutrinos. In this section, we also discuss finite temperature corrections from QED and comment on the computational method and initial conditions. In Sec. 3, we present our results of neutrino spectra and the value of N_{eff} for each basis. We also discuss the relation of distribution functions in the flavor and mass bases. Finally, we give our conclusions in Sec. 4. In appendices, the kinetic equations for neutrinos in comoving variables and analytic estimation of the collision integral are given.

2 Neutrino decoupling

2.1 Boltzmann equations in the flavor basis

In order to describe the process of neutrino decoupling in the early Universe, in particular, to estimate the spectral distortion with good precision, we first consider field operators of flavor neutrinos and their density matrices in a homogeneous system. In ultra-relativistic limit, the field operators of left-handed neutrinos are expanded as

$$\nu_\alpha(x) = \int \frac{d^3\mathbf{p}}{(2\pi)^3\sqrt{2p_0}} (a_\alpha(\mathbf{p}, t)u_{\mathbf{p}}e^{i\mathbf{p}\cdot\mathbf{x}} + b_\alpha^\dagger(\mathbf{p}, t)v_{\mathbf{p}}e^{-i\mathbf{p}\cdot\mathbf{x}}), \quad (1)$$

where $a_\alpha(\mathbf{p}, t) = a_\alpha(\mathbf{p})e^{-ip_0t}$ and $b_\alpha(\mathbf{p}, t) = b_\alpha(\mathbf{p})e^{-ip_0t}$ are annihilation operators for negative-helicity neutrinos and positive-helicity anti-neutrinos, respectively. α and \mathbf{p} are a flavor index and a three dimensional momentum with $p_0 \simeq |\mathbf{p}|$, respectively. $u_{\mathbf{p}}$ ($v_{\mathbf{p}}$) denotes the Dirac spinor for a massless negative-helicity particle (positive-helicity anti-particle), which is normalized to be $u_{\mathbf{p}}^\dagger u_{\mathbf{p}} = v_{\mathbf{p}}^\dagger v_{\mathbf{p}} = 2p_0$, and satisfies

$$\not{p}u_{\mathbf{p}} = 0, \quad \not{p}v_{\mathbf{p}} = 0. \quad (2)$$

These expansions of the field operators make sense only in the ultra-relativistic limit. The annihilation and creation operators satisfy the anti-commutation relations,

$$\{a_\alpha(\mathbf{p}), a_\beta^\dagger(\mathbf{p}')\} = \{b_\alpha(\mathbf{p}), b_\beta^\dagger(\mathbf{p}')\} = \delta_{\alpha\beta}(2\pi)^3\delta^{(3)}(\mathbf{p} - \mathbf{p}'). \quad (3)$$

The density matrices for neutrinos and anti-neutrinos are defined through the following expectation values of these operators with regard to the initial thermal equilibrium states,

$$\begin{aligned}\langle a_{\beta}^{\dagger}(\mathbf{p}, t) a_{\alpha}(\mathbf{p}', t) \rangle &= (2\pi)^3 \delta^{(3)}(\mathbf{p} - \mathbf{p}') (\rho_p)_{\alpha\beta}, \\ \langle b_{\alpha}^{\dagger}(\mathbf{p}, t) b_{\beta}(\mathbf{p}', t) \rangle &= (2\pi)^3 \delta^{(3)}(\mathbf{p} - \mathbf{p}') (\bar{\rho}_p)_{\alpha\beta},\end{aligned}\quad (4)$$

where $p = |\mathbf{p}|$. Due to the reversed order of flavor indices in $\bar{\rho}_p(t)$, both density matrices transform in the same way under a unitary transformation of flavor space. Here the diagonal parts are the usual distribution functions of flavor neutrinos and the off-diagonal parts are non-zero in the presence of flavor mixing. Note again that since the off-diagonal parts of the neutrino mass matrix are not zero, we cannot define annihilation operators, creation operators and density matrices for non-relativistic flavor neutrinos in the conventional way. In Sec. 2.2, we write field operators of neutrinos including their masses in the mass basis so that we can define density matrices for non-relativistic neutrinos.

The neutrino density matrix takes the following form,

$$\rho_p(t) = \begin{pmatrix} \rho_{ee} & \rho_{e\mu} & \rho_{e\tau} \\ \rho_{\mu e} & \rho_{\mu\mu} & \rho_{\mu\tau} \\ \rho_{\tau e} & \rho_{\tau\mu} & \rho_{\tau\tau} \end{pmatrix} = \begin{pmatrix} f_{\nu_e} & a_1 + ia_2 & b_1 + ib_2 \\ a_1 - ia_2 & f_{\nu_{\mu}} & c_1 + ic_2 \\ b_1 - ib_2 & c_1 - ic_2 & f_{\nu_{\tau}} \end{pmatrix}, \quad (5)$$

where $f_{\nu_{\alpha}}$ is the distribution function for flavor neutrinos and the off-diagonal parts are characterized by the real parameters a_i, b_i and c_i ($i = 1, 2$). Hereafter we neglect a neutrino asymmetry since neutrino oscillations leading to flavor equilibrium before BBN impose a stringent constraint on this asymmetry [19–21]. Under this assumption, neutrinos and anti-neutrinos satisfy the same density matrices and the same evolutions in the Universe, $\rho_p(t) = \bar{\rho}_p(t)^T$.

The equations of motion for the neutrino density matrix in the expanding Universe are [22, 23]

$$(\partial_t - Hp\partial_p)\rho_p(t) = -i \left[\left(\frac{M^2}{2p} - \frac{8\sqrt{2}G_F p}{3m_W^2} E \right), \rho_p(t) \right] + C[\rho_p(t)], \quad (6)$$

where H is the Hubble parameter, G_F is the Fermi coupling constant, m_W is the W boson mass, and $[\cdot, \cdot]$ represents the commutator of matrices with a flavor index. The first term¹ in the commutator is the vacuum oscillation term proportional to the mass-squared matrix in the flavor basis M^2 . The mass-squared matrix is related to the diagonal mass-squared matrix in the mass basis M_{diag}^2 through the Pontecorvo-Maki-Nakagawa-Sakata matrix,

¹Only when we derive the first term which comes from the free neutrino Hamiltonian including the mass matrix, we replace the operators $a_{\alpha}(\mathbf{p}, t)$ and $b_{\alpha}(\mathbf{p}, t)$ in Eq. (1) with $a_{\alpha}^{\text{osc}}(\mathbf{p}, t) = (\exp(-i\Omega_{\mathbf{p}}t))_{\alpha\beta} a_{\beta}(\mathbf{p})$ and $b_{\alpha}^{\text{osc}}(\mathbf{p}, t) = (\exp(-i\Omega_{\mathbf{p}}t))_{\alpha\beta} b_{\beta}(\mathbf{p})$ as in [22], where $\Omega_{\mathbf{p}} = \sqrt{\mathbf{p}^2 + M^2}$.

assuming the CP conservation,

$$\begin{aligned}
U_{\text{PMNS}} &\equiv \begin{pmatrix} U_{e1} & U_{e2} & U_{e3} \\ U_{\mu 1} & U_{\mu 2} & U_{\mu 3} \\ U_{\tau 1} & U_{\tau 2} & U_{\tau 3} \end{pmatrix}, \\
&= \begin{pmatrix} c_{12}c_{13} & s_{12}c_{13} & s_{13} \\ -s_{12}c_{23} - c_{12}s_{23}s_{13} & c_{12}c_{23} - s_{12}s_{23}s_{13} & s_{23}c_{13} \\ s_{12}s_{23} - c_{12}c_{23}s_{13} & -c_{12}s_{23} - s_{12}c_{23}s_{13} & c_{23}c_{13} \end{pmatrix}, \tag{7}
\end{aligned}$$

where $c_{ij} = \cos \theta_{ij}$ and $s_{ij} = \sin \theta_{ij}$ for $ij = 12, 13$, or 23 . The relation between the mass-squared matrices of neutrinos in the two bases is

$$\begin{aligned}
M_{\text{diag}}^2 &= U_{\text{PMNS}}^\dagger M^2 U_{\text{PMNS}}, \\
&= \text{diag}(m_1^2, m_2^2, m_3^2). \tag{8}
\end{aligned}$$

From the global analysis of neutrino oscillation experiments in [25], we consider the following best-fit values of neutrino masses and mixing parameters,

$$\begin{aligned}
\left(\frac{\Delta m_{21}^2}{10^{-5} \text{ eV}^2}, \frac{\Delta m_{31}^2}{10^{-3} \text{ eV}^2}, s_{12}^2, s_{23}^2, s_{13}^2 \right)_{\text{NH}} &= (7.39, 2.525, 0.310, 0.582, 0.0224), \\
\left(\frac{\Delta m_{21}^2}{10^{-5} \text{ eV}^2}, \frac{\Delta m_{31}^2}{10^{-3} \text{ eV}^2}, s_{12}^2, s_{23}^2, s_{13}^2 \right)_{\text{IH}} &= (7.39, -2.512, 0.310, 0.582, 0.02263), \tag{9}
\end{aligned}$$

where $\Delta m_{ij}^2 = m_i^2 - m_j^2$. The first (second) equation in Eq. (9) corresponds to the normal (inverted) hierarchy ordering of neutrino masses.

The second term in the commutator in Eq. (6) represents the refractive effect in the medium which comes from one-loop thermal contributions to the neutrino self-energy. The diagonal matrix E is the energy density of the charged leptons and in the temperature of MeV scale, E takes the following form approximately,

$$E = \text{diag}(\rho_{ee}, 0, 0), \tag{10}$$

where $\rho_{ee} = \rho_{e-} + \rho_{e+}$ is the energy density of electrons and positrons. We neglect other refractive terms coming from the charged lepton asymmetries and neutrino self-interactions, which are significantly suppressed [22, 24].

The final term in Eq. (6) represents the collisions of neutrinos with electrons, positrons, and themselves, which are dominated by two-body reactions $1 + 2 \rightarrow 3 + 4$. As done in the previously most accurate calculation of neutrino decoupling in the early Universe [17], we also deal with both diagonal and off-diagonal collision terms for the processes which involve electrons and positrons. On the other hand, we do not treat the off-diagonal terms for the self-interactions of neutrinos, such as $\nu\nu \leftrightarrow \nu\nu$ or $\nu\bar{\nu} \leftrightarrow \nu\bar{\nu}$ since the annihilations of electrons and positrons are important for the heating process of neutrinos while the self-interactions of neutrinos less contribute to this heating process.

The diagonal collision term from the self-interaction processes $\nu(p_1)\nu(p_2) \leftrightarrow \nu(p_3)\nu(p_4)$ and $\nu(p_1)\bar{\nu}(p_2) \leftrightarrow \nu(p_3)\bar{\nu}(p_4)$ is

$$\begin{aligned}
C_S[\nu_\alpha(p_1)] = & \frac{2^5 G_F^2}{2 |\mathbf{p}_1|} \int \frac{d^3 \mathbf{p}_2}{(2\pi)^3 2 |\mathbf{p}_2|} \frac{d^3 \mathbf{p}_3}{(2\pi)^3 2 |\mathbf{p}_3|} \frac{d^3 \mathbf{p}_4}{(2\pi)^3 2 |\mathbf{p}_4|} (2\pi)^4 \delta^{(4)}(p_1 + p_2 - p_3 - p_4) \\
& \times \left[\{4(p_1 \cdot p_4)(p_2 \cdot p_3) + 2(p_1 \cdot p_2)(p_3 \cdot p_4)\} F(\nu_\alpha^{(1)}, \nu_\alpha^{(2)}, \nu_\alpha^{(3)}, \nu_\alpha^{(4)}) \right. \\
& + \{(p_1 \cdot p_4)(p_2 \cdot p_3) + (p_1 \cdot p_2)(p_3 \cdot p_4)\} F(\nu_\alpha^{(1)}, \nu_\beta^{(2)}, \nu_\alpha^{(3)}, \nu_\beta^{(4)}) \\
& + (p_1 \cdot p_4)(p_2 \cdot p_3) F(\nu_\alpha^{(1)}, \nu_\alpha^{(2)}, \nu_\beta^{(3)}, \nu_\beta^{(4)}) \\
& + \{(p_1 \cdot p_4)(p_2 \cdot p_3) + (p_1 \cdot p_2)(p_3 \cdot p_4)\} F(\nu_\alpha^{(1)}, \nu_\gamma^{(2)}, \nu_\alpha^{(3)}, \nu_\gamma^{(4)}) \\
& \left. + (p_1 \cdot p_4)(p_2 \cdot p_3) F(\nu_\alpha^{(1)}, \nu_\alpha^{(2)}, \nu_\gamma^{(3)}, \nu_\gamma^{(4)}) \right], \tag{11}
\end{aligned}$$

where $\alpha, \beta, \gamma = e, \mu, \tau$ and $\alpha \neq \beta, \alpha \neq \gamma, \beta \neq \gamma$. We define $F(\nu_\alpha^{(1)}, \nu_\beta^{(2)}, \nu_\gamma^{(3)}, \nu_\delta^{(4)})$ as

$$\begin{aligned}
F(\nu_\alpha^{(1)}, \nu_\beta^{(2)}, \nu_\gamma^{(3)}, \nu_\delta^{(4)}) = & f_{\nu_\gamma}(p_3) f_{\nu_\delta}(p_4) (1 - f_{\nu_\alpha}(p_1)) (1 - f_{\nu_\beta}(p_2)) \\
& - f_{\nu_\alpha}(p_1) f_{\nu_\beta}(p_2) (1 - f_{\nu_\gamma}(p_3)) (1 - f_{\nu_\delta}(p_4)), \tag{12}
\end{aligned}$$

where $\alpha, \beta, \delta, \gamma = e, \mu, \tau$.

The collision term from the annihilation processes $\nu(p_1)\bar{\nu}(p_2) \leftrightarrow e^-(p_3)e^+(p_4)$ is

$$\begin{aligned}
C_A = & \frac{1}{2} \frac{2^5 G_F^2}{2 |\mathbf{p}_1|} \int \frac{d^3 \mathbf{p}_2}{(2\pi)^3 2 |\mathbf{p}_2|} \frac{d^3 \mathbf{p}_3}{(2\pi)^3 2 E_3} \frac{d^3 \mathbf{p}_4}{(2\pi)^3 2 E_4} (2\pi)^4 \delta^{(4)}(p_1 + p_2 - p_3 - p_4) \\
& \times \left[4(p_1 \cdot p_4)(p_2 \cdot p_3) F_A^{LL}(\nu^{(1)}, \bar{\nu}^{(2)}, e^{(3)}, \bar{e}^{(4)}) \right. \\
& + 4(p_1 \cdot p_3)(p_2 \cdot p_4) F_A^{RR}(\nu^{(1)}, \bar{\nu}^{(2)}, e^{(3)}, \bar{e}^{(4)}) \\
& \left. + 2(p_1 \cdot p_2) m_e^2 \left(F_A^{LR}(\nu^{(1)}, \bar{\nu}^{(2)}, e^{(3)}, \bar{e}^{(4)}) + F_A^{RL}(\nu^{(1)}, \bar{\nu}^{(2)}, e^{(3)}, \bar{e}^{(4)}) \right) \right], \tag{13}
\end{aligned}$$

where

$$\begin{aligned}
F_A^{ab}(\nu^{(1)}, \bar{\nu}^{(2)}, e^{(3)}, \bar{e}^{(4)}) = & f_e(p_3) f_e(p_4) \left(Y^a(1 - \bar{\rho}_2) Y^b(1 - \rho_1) + (1 - \rho_1) Y^b(1 - \bar{\rho}_2) Y^a \right) \\
& - (1 - f_e(p_3))(1 - f_e(p_4)) \left(Y^a \bar{\rho}_2 Y^b \rho_1 + \rho_1 Y^b \bar{\rho}_2 Y^a \right). \tag{14}
\end{aligned}$$

Here $f_e(p)$ is the distribution functions of electrons and positrons, and $\bar{\rho}_2 = \rho_2^T$. We assume that electrons and positrons are always in thermal equilibrium since electrons, positrons and photons interact with each other through rapid electromagnetic interactions. Under this assumption, the distribution functions of electrons and positrons take the following form,

$$f_e(p) = \frac{1}{\exp(\sqrt{p^2 + m_e^2}/T_\gamma) + 1}. \tag{15}$$

$Y^a (a = L, R)$ is a 3×3 matrix of couplings and becomes in the flavor basis

$$\begin{aligned} Y^L &= \text{diag}(g_L, \tilde{g}_L, \tilde{g}_L), \\ Y^R &= \text{diag}(g_R, g_R, g_R), \end{aligned} \quad (16)$$

where

$$g_L = \frac{1}{2} + \sin^2 \theta_W, \quad \tilde{g}_L = -\frac{1}{2} + \sin^2 \theta_W, \quad g_R = \sin^2 \theta_W. \quad (17)$$

Here $\sin^2 \theta_W \simeq 0.231$ and θ_W is the weak mixing angle.

The collision term from the scattering processes $\nu(p_1)e^-(p_2) \leftrightarrow \nu(p_3)e^-(p_4)$ and $\nu(p_1)e^+(p_2) \leftrightarrow \nu(p_3)e^+(p_4)$ is

$$\begin{aligned} C_{SC} &= \frac{1}{2} \frac{2^5 G_F^2}{2 |\mathbf{p}_1|} \int \frac{d^3 \mathbf{p}_2}{(2\pi)^3 2E_2} \frac{d^3 \mathbf{p}_3}{(2\pi)^3 2|\mathbf{p}_3|} \frac{d^3 \mathbf{p}_4}{(2\pi)^3 2E_4} (2\pi)^4 \delta^{(4)}(p_1 + p_2 - p_3 - p_4) \\ &\times \left[4 \{ (p_1 \cdot p_4)(p_2 \cdot p_3) + (p_1 \cdot p_2)(p_3 \cdot p_4) \} \right. \\ &\times \left(F_{SC}^{LL}(\nu^{(1)}, e^{(2)}, \nu^{(3)}, e^{(4)}) + F_{SC}^{RR}(\nu^{(1)}, e^{(2)}, \nu^{(3)}, e^{(4)}) \right) \\ &\left. - 4(p_1 \cdot p_3)m_e^2 \left(F_{SC}^{LR}(\nu^{(1)}, e^{(2)}, \nu^{(3)}, e^{(4)}) + F_{SC}^{RL}(\nu^{(1)}, e^{(2)}, \nu^{(3)}, e^{(4)}) \right) \right], \end{aligned} \quad (18)$$

where

$$\begin{aligned} F_{SC}^{ab}(\nu^{(1)}, e^{(2)}, \nu^{(3)}, e^{(4)}) &= f_e(p_4)(1 - f_e(p_2)) \left(Y^a \rho_3 Y^b (1 - \rho_1) + (1 - \rho_1) Y^b \rho_3 Y^a \right) \\ &- f_e(p_2)(1 - f_e(p_4)) \left(\rho_1 Y^b (1 - \rho_3) Y^a + Y^a (1 - \rho_3) Y^b \rho_1 \right). \end{aligned} \quad (19)$$

These collision terms are described in detail in appendix A.

In addition to the Boltzmann equations for the neutrino density matrix, the energy conservation law must be satisfied,

$$\frac{d\rho}{dt} = -3H(\rho + P), \quad (20)$$

where ρ and P are the total energy density and pressure of the standard model particles (γ, e^\pm, ν_i) respectively. Though we will discuss finite temperature corrections from QED to ρ, P and m_e later, in the ideal gas limit, they are given as follows, which are denoted by $\rho_{(0)}$ and $P_{(0)}$ respectively,

$$\begin{aligned} \rho_{(0)} &= \frac{\pi^2 T_\gamma^4}{15} + \frac{2}{\pi^2} \int \frac{dp p^2 \sqrt{p^2 + m_e^2}}{\exp(\sqrt{p^2 + m_e^2}/T_\gamma) + 1} + \sum_{\alpha=e, \mu, \tau} \frac{1}{\pi^2} \int dp p^3 f_{\nu_\alpha}(p), \\ P_{(0)} &= \frac{\pi^2 T_\gamma^4}{45} + \frac{2}{\pi^2} \int \frac{dp p^4}{3\sqrt{p^2 + m_e^2} [\exp(\sqrt{p^2 + m_e^2}/T_\gamma) + 1]} + \sum_{\alpha=e, \mu, \tau} \frac{1}{3\pi^2} \int dp p^3 f_{\nu_\alpha}(p). \end{aligned} \quad (21)$$

The energy conservation law governs the evolution of the photon temperature T_γ . The Hubble parameter in Eqs. (6) and (20) is calculated using the usual relation, $3H^2 m_{\text{Pl}}^2 = 8\pi\rho$ with m_{Pl} being the Planck mass, where we ignore the curvature term and the cosmological constant because they are negligible in the radiation dominated epoch.

2.2 Boltzmann equations in the mass basis

In this section, we formulate the Boltzmann equations for the density matrices of massive neutrinos at the early Universe in the mass basis. If we would like to observe the distortions of neutrinos in the current Universe in future, it is easier to follow the evolution of negative-helicity neutrinos in the diagonal mass basis since the helicity states of neutrinos are conserved while non-relativistic neutrinos are freely streaming. Thus, it is quite useful to formulate the Boltzmann equations for negative-helicity neutrinos in the mass basis though we concentrate on neutrino decoupling processes in this paper, where ultra-relativistic limit is a good approximation and there are no much difference between the two bases. This approach is also complementary to that in the flavor basis given in the previous subsection 2.1 and is useful for the cross-check of the results.

Since the negative-helicity neutrinos in the mass basis satisfy the free Dirac equation, they are expanded as

$$\nu_i(x) = \int \frac{d^3\mathbf{p}}{(2\pi)^3 \sqrt{2E_i}} \left(a_i(\mathbf{p}, t) u_{\mathbf{p}}^{(i)} e^{i\mathbf{p}\cdot\mathbf{x}} + b_i^\dagger(\mathbf{p}, t) v_{\mathbf{p}}^{(i)} e^{-i\mathbf{p}\cdot\mathbf{x}} \right), \quad (22)$$

where $i(=1, 2, 3)$ represents a mass eigenstate, $a_i(\mathbf{p}, t) = a_i(\mathbf{p}) e^{-iE_i t}$, $b_i(\mathbf{p}, t) = b_i(\mathbf{p}) e^{-iE_i t}$, $E_i = \sqrt{\mathbf{p}^2 + m_i^2}$ and m_i is the neutrino mass in the mass basis. Since $u_{\mathbf{p}}^{(i)}$ ($v_{\mathbf{p}}^{(i)}$) denotes the Dirac spinor for massive negative-helicity particles (positive-helicity anti-particles), which is also normalized to be $u_{\mathbf{p}}^{(i)\dagger} u_{\mathbf{p}}^{(i)} = v_{\mathbf{p}}^{(i)\dagger} v_{\mathbf{p}}^{(i)} = 2E_i$, the Dirac spinors satisfy

$$(\not{p} - m_i) u_{\mathbf{p}}^{(i)} = 0, \quad (\not{p} + m_i) v_{\mathbf{p}}^{(i)} = 0. \quad (23)$$

As in the flavor basis, $a_i(\mathbf{p})$ and $b_i(\mathbf{p})$ are annihilation operators for negative-helicity neutrinos and for positive-helicity anti-neutrinos in the mass basis, respectively, which satisfy

$$\{a_i(\mathbf{p}), a_j^\dagger(\mathbf{p}')\} = \{b_i(\mathbf{p}), b_j^\dagger(\mathbf{p}')\} = \delta_{ij} (2\pi)^3 \delta^{(3)}(\mathbf{p} - \mathbf{p}'). \quad (24)$$

The density matrices for neutrinos and anti-neutrinos in the mass basis are given by

$$\begin{aligned} \langle a_j^\dagger(\mathbf{p}, t) a_i(\mathbf{p}', t) \rangle &= (2\pi)^3 \delta^{(3)}(\mathbf{p} - \mathbf{p}') (\rho_p)_{ij}, \\ \langle b_i^\dagger(\mathbf{p}, t) b_j(\mathbf{p}', t) \rangle &= (2\pi)^3 \delta^{(3)}(\mathbf{p} - \mathbf{p}') (\bar{\rho}_p)_{ij}, \end{aligned} \quad (25)$$

where the diagonal parts are the distribution functions for massive neutrinos.

In the following, we study the kinetic equations for the neutrino density matrix in ultra-relativistic limit. In this limit, negative-helicity neutrinos coincide with left-handed neutrinos due to no distinction between helicity and chirality. The diagonalization of mass

matrix for left-handed neutrinos in the flavor basis is achieved through the transformations,

$$\boldsymbol{\nu}_\alpha(x) = \sum_{i=1}^3 U_{\alpha i} \boldsymbol{\nu}_i(x), \quad (26)$$

with $\alpha = e, \mu, \tau$. Here $U_{\alpha i}$ represents a component of the unitary matrix U_{PMNS} given in Eq. (7).

In order to specify the collision processes for massive neutrinos, we discuss weak neutral currents and charged currents in the mass basis. The weak neutral currents of electrons, positrons, and neutrinos are

$$J_{\text{NC}}^\mu = J_{ee}^{L\mu} + J_{ee}^{R\mu} + J_{\nu\nu}^\mu, \quad (27)$$

where $J_{ee}^{L\mu}$ and $J_{ee}^{R\mu}$ are the neutral currents of left-handed electrons and right-handed electrons respectively and given by

$$\begin{aligned} J_{ee}^{L\mu} &= \tilde{g}_L \bar{e} \gamma^\mu (1 - \gamma_5) e, \\ J_{ee}^{R\mu} &= g_R \bar{e} \gamma^\mu (1 + \gamma_5) e, \end{aligned} \quad (28)$$

where e is the field operator of electron. The neutral currents for the left-handed neutrinos in both bases are given by the following form and they are related through the unitary U_{PMNS} matrix,

$$J_{\nu\nu}^\mu = \sum_{\alpha=e,\mu,\tau} \bar{\nu}_\alpha \gamma^\mu (1 - \gamma_5) \nu_\alpha = \sum_{i=1,2,3} \bar{\nu}_i \gamma^\mu (1 - \gamma_5) \nu_i. \quad (29)$$

The charged currents for left-handed electrons and left-handed electron neutrinos are given by

$$J_{e\nu_e}^\mu = \bar{\nu}_e \gamma^\mu (1 - \gamma_5) e. \quad (30)$$

Using the Fierz transformations for fermionic fields, we can describe the Hamiltonian density including the charged currents at the neutrino decoupling process as

$$\begin{aligned} \mathcal{H}_{CC} &= \frac{G_F}{\sqrt{2}} J_{e\nu_e}^{\dagger\mu} (J_{e\nu_e})_\mu = \frac{G_F}{\sqrt{2}} J_{ee}^{L\mu} (J_{\nu_e\nu_e})_\mu, \\ J_{\nu_e\nu_e}^\mu &= \bar{\nu}_e \gamma^\mu (1 - \gamma_5) \nu_e. \end{aligned} \quad (31)$$

Since Eq. (31) implies that the charged currents in the Hamiltonian density \mathcal{H}_{CC} can be replaced by the equivalent neutral currents, we implicitly take the charged currents into account by making the following replacement of the coefficient of neutral currents for electron neutrinos in the collision terms,

$$\tilde{g}_L \rightarrow g_L = \tilde{g}_L + 1. \quad (32)$$

In the mass basis, the charged currents for neutrinos and electrons are, through the U_{PMNS} matrix,

$$\begin{aligned} J_{e\nu_e}^\mu &= \bar{\nu}_e \gamma^\mu (1 - \gamma_5) e, \\ &= \sum_{i=1}^3 U_{ei}^* \bar{\nu}_i \gamma^\mu (1 - \gamma_5) e. \end{aligned} \quad (33)$$

The replacement in Eq. (31) corresponds to the following relation in the mass basis,

$$\begin{aligned} J_{e\nu_e}^{\dagger\mu} (J_{e\nu_e})_\mu &= \sum_{i=1}^3 \sum_{j=1}^3 U_{ei}^* U_{ej} J_{ee}^{L\mu} (J_{\nu_i \nu_j})_\mu, \\ J_{\nu_i \nu_j}^\mu &= \bar{\nu}_i \gamma^\mu (1 - \gamma_5) \nu_j. \end{aligned} \quad (34)$$

From the above equation, the corresponding couplings to Y^a in Eqs. (14) and (19) are changed into

$$\begin{aligned} Y^L &\rightarrow Z^L = \begin{pmatrix} \tilde{g}_L + U_{e1}^* U_{e1} & U_{e1}^* U_{e2} & U_{e1}^* U_{e3} \\ U_{e2}^* U_{e1} & \tilde{g}_L + U_{e2}^* U_{e2} & U_{e2}^* U_{e3} \\ U_{e3}^* U_{e1} & U_{e3}^* U_{e2} & \tilde{g}_L + U_{e3}^* U_{e3} \end{pmatrix}, \\ Y^R &\rightarrow Z^R = Y^R = \text{diag}(g_R, g_R, g_R). \end{aligned} \quad (35)$$

The collision term from the self-interaction processes in the mass basis takes the same form as that in the flavor basis except for the subscripts,

$$\begin{aligned} C_S[\nu_i(p_1)] &= \frac{2^5 G_F^2}{2 |\mathbf{p}_1|} \int \frac{d^3 \mathbf{p}_2}{(2\pi)^3 2 |\mathbf{p}_2|} \frac{d^3 \mathbf{p}_3}{(2\pi)^3 2 |\mathbf{p}_3|} \frac{d^3 \mathbf{p}_4}{(2\pi)^3 2 |\mathbf{p}_4|} (2\pi)^4 \delta^{(4)}(p_1 + p_2 - p_3 - p_4) \\ &\times \left[\{4(p_1 \cdot p_4)(p_2 \cdot p_3) + 2(p_1 \cdot p_2)(p_3 \cdot p_4)\} F(\nu_i^{(1)}, \nu_i^{(2)}, \nu_i^{(3)}, \nu_i^{(4)}) \right. \\ &+ \{(p_1 \cdot p_4)(p_2 \cdot p_3) + (p_1 \cdot p_2)(p_3 \cdot p_4)\} F(\nu_i^{(1)}, \nu_j^{(2)}, \nu_i^{(3)}, \nu_j^{(4)}) \\ &+ (p_1 \cdot p_4)(p_2 \cdot p_3) F(\nu_i^{(1)}, \nu_i^{(2)}, \nu_j^{(3)}, \nu_j^{(4)}) \\ &+ \{(p_1 \cdot p_4)(p_2 \cdot p_3) + (p_1 \cdot p_2)(p_3 \cdot p_4)\} F(\nu_i^{(1)}, \nu_k^{(2)}, \nu_i^{(3)}, \nu_k^{(4)}) \\ &\left. + (p_1 \cdot p_4)(p_2 \cdot p_3) F(\nu_i^{(1)}, \nu_i^{(2)}, \nu_k^{(3)}, \nu_k^{(4)}) \right], \end{aligned} \quad (36)$$

where $i, j, k = 1, 2, 3$ and $i \neq j, i \neq k, j \neq k$. The collision term from the annihilation processes is

$$\begin{aligned} C_A &= \frac{1}{2} \frac{2^5 G_F^2}{2 |\mathbf{p}_1|} \int \frac{d^3 \mathbf{p}_2}{(2\pi)^3 2 |\mathbf{p}_2|} \frac{d^3 \mathbf{p}_3}{(2\pi)^3 2 E_3} \frac{d^3 \mathbf{p}_4}{(2\pi)^3 2 E_4} (2\pi)^4 \delta^{(4)}(p_1 + p_2 - p_3 - p_4) \\ &\times \left[4(p_1 \cdot p_4)(p_2 \cdot p_3) G_A^{LL}(\nu^{(1)}, \bar{\nu}^{(2)}, e^{(3)}, \bar{e}^{(4)}) \right. \\ &+ 4(p_1 \cdot p_3)(p_2 \cdot p_4) G_A^{RR}(\nu^{(1)}, \bar{\nu}^{(2)}, e^{(3)}, \bar{e}^{(4)}) \\ &\left. + 2(p_1 \cdot p_2) m_e^2 \left(G_A^{LR}(\nu^{(1)}, \bar{\nu}^{(2)}, e^{(3)}, \bar{e}^{(4)}) + G_A^{RL}(\nu^{(1)}, \bar{\nu}^{(2)}, e^{(3)}, \bar{e}^{(4)}) \right) \right], \end{aligned} \quad (37)$$

where

$$\begin{aligned}
G_A^{ab}(\nu^{(1)}, \bar{\nu}^{(2)}, e^{(3)}, \bar{e}^{(4)}) \\
= f_e(p_3)f_e(p_4)\left(Z^a(1-\bar{\rho}_2)Z^b(1-\rho_1) + (1-\rho_1)Z^b(1-\bar{\rho}_2)Z^a\right) \\
- (1-f_e(p_3))(1-f_e(p_4))\left(Z^a\bar{\rho}_2Z^b\rho_1 + \rho_1Z^b\bar{\rho}_2Z^a\right). \tag{38}
\end{aligned}$$

The collision term from the scattering processes is

$$\begin{aligned}
C_{SC} = & \frac{1}{2} \frac{2^5 G_F^2}{2|\mathbf{p}_1|} \int \frac{d^3\mathbf{p}_2}{(2\pi)^3 2E_2} \frac{d^3\mathbf{p}_3}{(2\pi)^3 2|\mathbf{p}_3|} \frac{d^3\mathbf{p}_4}{(2\pi)^3 2E_4} (2\pi)^4 \delta^{(4)}(p_1 + p_2 - p_3 - p_4) \\
& \times \left[4\{(p_1 \cdot p_4)(p_2 \cdot p_3) + (p_1 \cdot p_2)(p_3 \cdot p_4)\} \right. \\
& \times \left(G_{SC}^{LL}(\nu^{(1)}, e^{(2)}, \nu^{(3)}, e^{(4)}) + G_{SC}^{RR}(\nu^{(1)}, e^{(2)}, \nu^{(3)}, e^{(4)}) \right) \\
& \left. - 4(p_1 \cdot p_3)m_e^2 \left(G_{SC}^{LR}(\nu^{(1)}, e^{(2)}, \nu^{(3)}, e^{(4)}) + G_{SC}^{RL}(\nu^{(1)}, e^{(2)}, \nu^{(3)}, e^{(4)}) \right) \right], \tag{39}
\end{aligned}$$

where

$$\begin{aligned}
G_{SC}^{ab}(\nu^{(1)}, e^{(2)}, \nu^{(3)}, e^{(4)}) \\
= f_e(p_4)(1-f_e(p_2))\left(Z^a\rho_3Z^b(1-\rho_1) + (1-\rho_1)Z^b\rho_3Z^a\right) \\
- f_e(p_2)(1-f_e(p_4))\left(\rho_1Z^b(1-\rho_3)Z^a + Z^a(1-\rho_3)Z^b\rho_1\right). \tag{40}
\end{aligned}$$

Finally, the equations of motion for the neutrino density matrix in the mass basis are given by

$$(\partial_t - Hp\partial_p)\rho_p(t) = -i \left[\left(\frac{M_{\text{diag}}^2}{2p} - \frac{8\sqrt{2}G_F p}{3m_W^2} \tilde{E} \right), \rho_p(t) \right] + C[\rho_p(t)]. \tag{41}$$

Since \tilde{E} and E are the thermal contributions to the self-energies of left-handed neutrinos, these have the same relation as that of M_{diag}^2 and M^2 , which is given by,

$$\tilde{E} = U_{\text{PMNS}}^\dagger E U_{\text{PMNS}}. \tag{42}$$

2.3 Finite temperature corrections from QED

In this section, we discuss finite temperature corrections from QED up to the next-to-leading order $\mathcal{O}(e^3)$, which modify electron, positron and photon masses. Through these corrections, several points in the former sections are changed. First, the modification of masses affects the energy density and the pressure of the electromagnetic plasma, and the collision rates involving electron and positrons. In addition, the expansion rate H in the Boltzmann equations changes through the total energy density of the plasma.

The corrections to electron, positron and photon masses can be obtained perturbatively by calculating the loop corrections to the self-energies of these particles. The

corrections to the electron and positron masses from finite temperature effects at $\mathcal{O}(e^2)$ are given by [26],

$$\begin{aligned} \delta m_{e(2)}^2(p, T_\gamma) = & \frac{2\pi\alpha T_\gamma^2}{3} + \frac{4\alpha}{\pi} \int_0^\infty dk \frac{k^2}{E_k} \frac{1}{\exp(E_k/T_\gamma) + 1} \\ & - \frac{2m_e^2\alpha}{\pi p} \int_0^\infty dk \frac{k}{E_k} \log \left| \frac{p+k}{p-k} \right| \frac{1}{\exp(E_k/T_\gamma) + 1}, \end{aligned} \quad (43)$$

where $\alpha = e^2/4\pi$ and $E_k = \sqrt{k^2 + m_e^2}$. The last term gives less than a 10% correction to $\delta m_{e(2)}^2$ around the decoupling temperature and the average momentum of electron [27], and contributes about 0.00005 to N_{eff} in the instantaneous decoupling limit [28]. Due to this smallness, we neglect the last term and consider only the first two terms, which depend only on T_γ . On the other hand, the thermal corrections to the photon mass at $\mathcal{O}(e^2)$ is given by [10],

$$\delta m_{\gamma(2)}^2(T_\gamma) = \frac{8\alpha}{\pi} \int_0^\infty dk \frac{k^2}{E_k} \frac{1}{\exp(E_k/T_\gamma) + 1}. \quad (44)$$

The total pressure and the total energy density of the electromagnetic plasma are given by, including thermal mass corrections of electrons, positrons and photons,

$$\begin{aligned} P = & \frac{T_\gamma}{\pi^2} \int_0^\infty dk \, k^2 \log \left[\frac{(1 + e^{-E_e/T_\gamma})^2}{(1 - e^{-E_\gamma/T_\gamma})} \right], \\ \rho = & -P + T_\gamma \frac{dP}{dT_\gamma}, \end{aligned} \quad (45)$$

where $E_\gamma = \sqrt{k^2 + \delta m_\gamma^2}$ and $E_e = \sqrt{k^2 + m_e^2 + \delta m_e^2}$. δm_γ^2 and δm_e^2 denote the thermal mass corrections of photons and electrons, respectively. We expand P in terms of δm_e^2 and δm_γ^2 at $\mathcal{O}(e^2)$ and get the leading order correction to the pressure [11],

$$P_{(2)} = - \int_0^\infty \frac{dk}{2\pi^2} \left[\frac{k^2}{E_k} \frac{\delta m_{e(2)}^2}{\exp(E_k/T_\gamma) + 1} + \frac{k}{2} \frac{\delta m_{\gamma(2)}^2}{\exp(k/T_\gamma) - 1} \right]. \quad (46)$$

Here we need to introduce the symmetry factor 1/2 in Eq. (46) in order to avoid the double counting of the thermal corrections to the total pressure. Then the leading order correction to the energy density is obtained as

$$\rho_{(2)} = -P_{(2)} + T_\gamma \frac{dP_{(2)}}{dT_\gamma}. \quad (47)$$

The next-to-leading order of thermal corrections to the photon mass is $\mathcal{O}(e^3)$. These nontrivial corrections to the photon mass come from the resummation of ring diagrams at all orders. Through this mass correction, the thermal corrections to the pressure and energy density are given by [28],

$$\begin{aligned} P_{(3)} = & \frac{e^3 T_\gamma}{12\pi^4} I^{3/2}(T_\gamma), \\ \rho_{(3)} = & \frac{e^3 T_\gamma^2}{8\pi^4} I^{1/2} \partial_{T_\gamma} I, \end{aligned} \quad (48)$$

where

$$I(T_\gamma) = 2 \int_0^\infty dk \left(\frac{k^2 + E_k^2}{E_k} \right) \frac{1}{\exp(E_k/T_\gamma) + 1}. \quad (49)$$

Note that the thermal corrections at $\mathcal{O}(e^3)$ do not modify the collision terms since these corrections change only the photon mass while the next corrections to the electron mass would appear at $\mathcal{O}(e^4)$. Finally, we read the total energy density and the total pressure of the electromagnetic plasma as

$$\begin{aligned} P &= P_{(0)} + P_{(2)} + P_{(3)}, \\ \rho &= \rho_{(0)} + \rho_{(2)} + \rho_{(3)}. \end{aligned} \quad (50)$$

2.4 Computational method and initial conditions

We solve a set of Eqs. (6) and (20) with the following comoving variables instead of the cosmic time t , a momentum p , and the photon temperature T_γ ,

$$x = m_e a, \quad y = pa, \quad z = T_\gamma a, \quad (51)$$

where we take an arbitrary mass scale to be the electron mass m_e and a is the scale factor of the Universe, normalized as $z \rightarrow 1$ in the high temperature limit.

Since the Boltzmann equations (6) are integro-differential equations due to the collision terms, these equations were solved by a discretization in a grid of comoving momenta y_i in refs. [6–8, 13, 16–18], by an expansion of the distortions of neutrinos in moments in refs. [9, 11, 12], or by a hybrid method combining the former two methods in ref. [15]. In this study, we use the former discretization method and take 100 grid points for the comoving momentum, equally spaced in the region $y_i \in [0.02, 20]$.

We have numerically calculated the evolution of the density matrix and the photon temperature in the interval $x_{\text{in}} \leq x \leq x_f$. We have chosen $x_{\text{in}} = m_e/10$ MeV as an initial time. Since neutrinos keep in thermal equilibrium with the electromagnetic plasma at x_{in} , the initial values of density matrix $\rho_{y_i}^{\text{in}}(x)$ are,

$$\rho_{y_i}^{\text{in}}(x) = \text{diag} \left(\frac{1}{e^{y_i/z_{\text{in}}} + 1}, \frac{1}{e^{y_i/z_{\text{in}}} + 1}, \frac{1}{e^{y_i/z_{\text{in}}} + 1} \right). \quad (52)$$

The initial value of the dimensionless photon temperature at x_{in} , z_{in} , slightly differs from unity because of the finite electron and positron masses. Due to the entropy conservation of electromagnetic plasma, neutrinos and anti-neutrinos, z_{in} is set as in [8],

$$z_{\text{in}} = 1.00003. \quad (53)$$

We set $x_f = 30$ as a final time, when the neutrino density matrix and z can be regarded as frozen.

3 Results

3.1 The flavor basis

First, we have numerically solved a set of Eqs. (6) and (20) in the flavor basis, during the process of neutrino decoupling. In order to compare with previous results, we discuss the cases with and without neutrino mixing, and those with and without finite temperature corrections from QED up to $\mathcal{O}(e^2)$ and $\mathcal{O}(e^3)$. In the case with neutrino mixing, we also consider the normal neutrino mass hierarchy with the latest best-fit values of neutrino mixing parameters. Although we have considered the inverted mass hierarchy too, the results are almost the same in the case of normal mass hierarchy as in ref. [17]. Hereafter we only show the case of the normal mass hierarchy.

In Figs. 1 and 2, we show the evolution of the photon temperature and the distortions of the flavor neutrino spectra for a comoving momentum ($y = 5$) in the case with QED corrections up to $\mathcal{O}(e^3)$ respectively, where we plot the comoving photon temperature $z(x)$ and the neutrino spectra $f_{\nu_\alpha}/f_{\text{eq}}$ ($f_{\text{eq}} = [\exp(y) + 1]^{-1}$) as a function of the normalized cosmic scale factor x . At high temperature with ($x \lesssim 0.2$), the temperature differences between photons and neutrinos are negligible and neutrinos are in thermal equilibrium with electrons and positrons. In the intermediate regime with ($0.2 \lesssim x \lesssim 4$), weak interactions gradually become ineffective with shifting from small to large momenta. In this period, the neutrino spectra are distorted since the energies of electrons and positrons partially convert into those of neutrinos coupled with electromagnetic plasma. Finally, at low temperature with ($x > 4$), the collision term $C[\rho_p(t)]$ becomes ineffective and the distortions are frozen.

In Fig. 2, we show the results of the two cases with and without neutrino mixing. We find that the final values of $f_{\nu_\alpha}[y = 5]$ without flavor mixing are 1.17% for ν_e and 0.500% for $\nu_{\mu,\tau}$ larger than those in the instantaneous decoupling limit, that is, $f_{\text{eq}}[y = 5]$. This difference between electron-type neutrinos and mu(tau)-type neutrinos arises from the fact that only electron-type neutrinos interact with electrons and positrons through the weak charged-currents. On the other hand, in the cases with neutrino mixing, neutrino oscillations mix the distortions of the flavor neutrinos too. Though the flavor oscillation effects are subdominant to the refractive effects in the period with ($x \lesssim 0.2$), the refractive term gets ineffective in the lower temperature due to the annihilations of electrons and positrons. Thus, the oscillation terms finally mix the flavor neutrino distortions. We also find that the final values of $f_{\nu_\alpha}[y = 5]$ with flavor mixing are 0.895% for ν_e , 0.648% for ν_μ and 0.663% for ν_τ larger than those in the instantaneous decoupling limit, that is, $f_{\text{eq}}[y = 5]$.

In Fig. 3, we show the frozen values of the flavor neutrino spectra $f_{\nu_\alpha}/f_{\text{eq}}$ as a function of a comoving momentum y for both cases with and without neutrino mixing, including QED corrections up to $\mathcal{O}(e^3)$. This figure shows the fact that neutrinos with higher energies interact with electrons and positrons until a later epoch. In addition, we see that neutrino oscillations tend to equilibrate the flavor neutrino distortions. Although the neutrino spectra $f_{\nu_\alpha}/f_{\text{eq}}$ with low energies are very slightly less than unity, these extractions of low energy neutrinos stem from an energy boost through the scattering

by electrons, positrons, (and neutrinos) with sufficiently high energies, which are not yet annihilated and hence still effective at the neutrino decoupling process.

Finally, we give several important quantities characterizing the decoupling process of neutrinos. In Tables. 1 and 2, we give final values (at $x_f = 30$) of the dimensionless photon temperature z_{fin} , the difference of energy densities and number densities of flavor neutrinos from those in the instantaneous decoupling limit denoted by ρ_{ν_0} and n_{ν_0} , and the effective number of neutrinos N_{eff} defined as

$$\rho_r = \left[1 + \frac{7}{8} \left(\frac{4}{11} \right)^{4/3} N_{\text{eff}} \right] \rho_\gamma. \quad (54)$$

Here ρ_r and ρ_γ are the energy densities of the total radiations and photons, respectively. The effective number of neutrinos N_{eff} can be rewritten,

$$N_{\text{eff}} = \left(\frac{z_0}{z_{\text{fin}}} \right)^4 \left(3 + \frac{\delta\rho_{\nu_e}}{\rho_{\nu_0}} + \frac{\delta\rho_{\nu_\mu}}{\rho_{\nu_0}} + \frac{\delta\rho_{\nu_\tau}}{\rho_{\nu_0}} \right), \quad (55)$$

where $z_0 = (11/4)^{1/3} \simeq 1.40102$ is the final value of the dimensionless photon temperature in the instantaneous decoupling limit and $\delta\rho_{\nu_\alpha} = \rho_{\nu_\alpha} - \rho_{\nu_0}$.

Without neutrino mixing, we find the final values of N_{eff} are 3.03404 for the case without QED corrections and 3.04430 for the case with those up to $\mathcal{O}(e^2)$, which agree with recent previous works [12, 14, 15]. In addition, our results for the case without neutrino mixing but with QED corrections up to $\mathcal{O}(e^3)$ show that the final value of N_{eff} is slightly modified to 3.04335. Thus, the difference with QED corrections up to $\mathcal{O}(e^2)$ and $\mathcal{O}(e^3)$ (but without neutrino mixing) is 0.00095 in terms of N_{eff} , which is very close to the value estimated in the instantaneous decoupling limit [28].

In the cases with neutrino mixing, Table. 2 shows that the energy densities of μ, τ -type neutrinos increase more while those of electron-type neutrinos increase less, compared to the cases without neutrino mixing. This modification leads to the enhancement of the total energy density for neutrinos with final values of $N_{\text{eff}} = 3.04486$ with QED corrections up to $\mathcal{O}(e^2)$ and $N_{\text{eff}} = 3.04391$ with QED corrections up to $\mathcal{O}(e^3)$. Since the blocking factor for electron neutrinos, $(1 - f_{\nu_e})$, is decreased by neutrino mixing, the annihilation of electrons and positrons into electron neutrinos increases. Although the annihilation into the other neutrinos decreases, electron neutrinos contribute to the neutrino heating most efficiently, and neutrino oscillations enhance the annihilation of electrons and positrons into neutrinos. From these processes, we conclude that neutrino oscillations slightly promote neutrino heating and the difference of N_{eff} is 0.00056, which agrees with the results of previous works [17, 29, 30]. In this case, we also find that the difference of N_{eff} between the cases including QED corrections up to $\mathcal{O}(e^2)$ and $\mathcal{O}(e^3)$ is 0.00095.

Case	z_{fin}	N_{eff}
Instantaneous decoupling	1.40102	3.000
No mixing + No QED	1.39910	3.034
No mixing + QED up to $\mathcal{O}(e^2)$	1.39789	3.044
No mixing + QED up to $\mathcal{O}(e^3)$	1.39800	3.043
mixing + QED up to $\mathcal{O}(e^2)$	1.39786	3.045
mixing + QED up to $\mathcal{O}(e^3)$	1.39797	3.044

Table 1: The final values of comoving photon temperature and the effective number of neutrinos for flavor neutrinos in several cases.

Case	$\delta\bar{\rho}_{\nu_e}(\%)$	$\delta\bar{\rho}_{\nu_\mu}(\%)$	$\delta\bar{\rho}_{\nu_\tau}(\%)$	$\delta\bar{n}_{\nu_e}(\%)$	$\delta\bar{n}_{\nu_\mu}(\%)$	$\delta\bar{n}_{\nu_\tau}(\%)$
Instantaneous decoupling	0	0	0	0	0	0
No mixing + No QED	0.949	0.397	0.397	0.583	0.240	0.240
No mixing + QED up to $\mathcal{O}(e^2)$	0.937	0.391	0.391	0.575	0.236	0.236
No mixing + QED up to $\mathcal{O}(e^3)$	0.937	0.391	0.391	0.575	0.236	0.236
mixing + QED up to $\mathcal{O}(e^2)$	0.712	0.511	0.523	0.435	0.311	0.319
mixing + QED up to $\mathcal{O}(e^3)$	0.712	0.511	0.523	0.436	0.312	0.319

Table 2: The final values of the distortions of energy densities $\delta\bar{\rho}_{\nu_\alpha} \equiv \delta\rho_{\nu_\alpha}/\rho_{\nu_0}$ and number densities $\delta\bar{n}_{\nu_\alpha} \equiv (n_{\nu_\alpha} - n_{\nu_0})/n_{\nu_0}$ for flavor neutrinos in several cases.

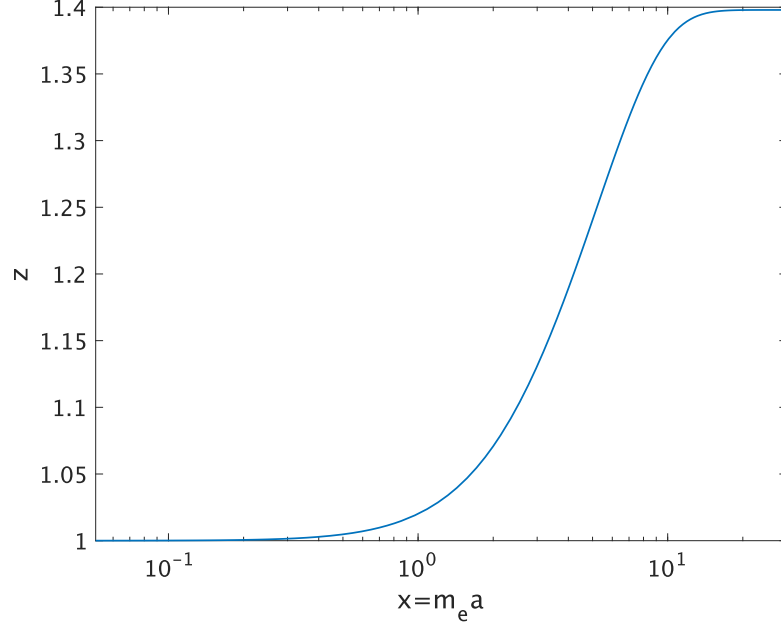


Figure 1: The time evolution of the comoving photon temperature $z(x)$ as a function of the normalized scale factor $x = m_e a$ in the case both with neutrino mixing and QED finite temperature corrections up to $\mathcal{O}(e^3)$.

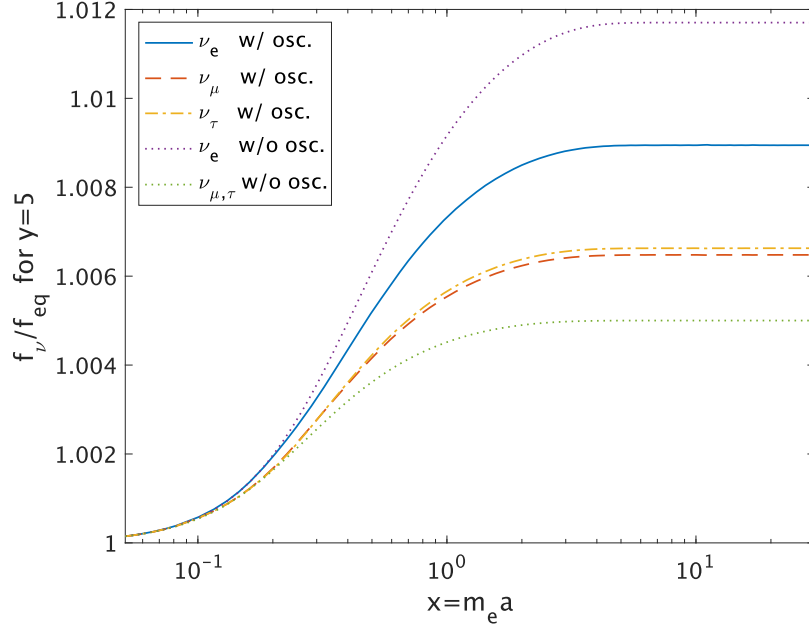


Figure 2: The time evolution of the distortions of flavor neutrinos for a fixed momentum ($y = 5$) as a function of the normalized scale factor $x = m_e a$ in the case with QED finite temperature corrections up to $\mathcal{O}(e^3)$. Upper (lower) dotted line is for ν_e ($\nu_{\mu,\tau}$) without neutrino oscillations. Inner three lines are for flavor neutrinos with neutrino oscillations.

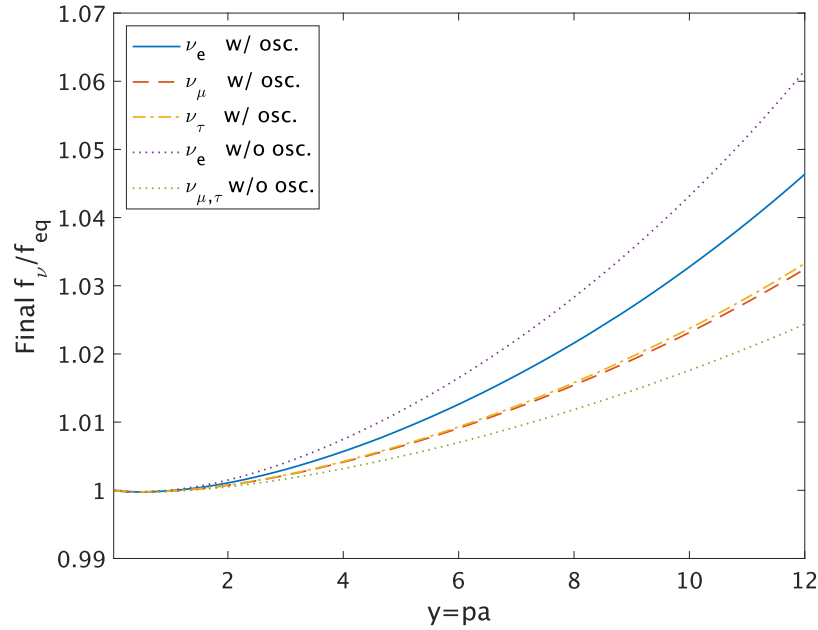


Figure 3: The final distortions of flavor neutrino spectra as a function of the comoving momentum y in the case with QED finite temperature corrections up to $\mathcal{O}(e^3)$. Dotted lines represent those for ν_e ($\nu_{\mu,\tau}$) without neutrino oscillations, while solid and dashed lines represent those for flavor neutrinos with neutrino oscillations.

3.2 The mass basis

In this section, we present the results of numerical calculations with a set of Eqs. (20) and (41). In the mass basis, we have also solved these equations with and without QED finite temperature corrections up to $\mathcal{O}(e^2)$ and $\mathcal{O}(e^3)$. Also in the mass basis, we show only the case of the normal mass hierarchy with the best-fit values of mixing parameters of neutrinos since we have checked that the results in the normal and inverted hierarchies are almost the same.

In Fig. 4, we show that the evolution of the massive neutrino spectra, f_{ν_i}/f_{eq} , for a comoving momentum ($y = 5$) as a function of the normalized scale factor x with QED corrections up to $\mathcal{O}(e^3)$. The final values of $f_{\nu_i}[y = 5]$ are found to be 0.958% for ν_1 , 0.724% for ν_2 , and 0.522% for ν_3 larger than those in the instantaneous decoupling limit, $f_{\text{eq}}[y = 5]$. These differences of distortions arise since each massive neutrino interacts with electrons and positrons through the different coupling Z^L in Eq. (35) and the refractive effects in the mass basis generate the off-diagonal parts of the mass matrix for massive neutrinos effectively. In Fig. 5, we show the asymptotic values of the massive neutrino spectra f_{ν_i}/f_{eq} as a function of y with QED corrections up to $\mathcal{O}(e^3)$.

In Tables. 3 and 4, we also show that the final values of the dimensionless photon temperature z_{fin} , the energy densities $\rho_{\nu_i}/\rho_{\nu_0}$ and number densities n_{ν_i}/n_{ν_0} of massive neutrinos, and the effective number of neutrinos N_{eff} . For the cases with finite temperature corrections up to $\mathcal{O}(e^2)$ and $\mathcal{O}(e^3)$, we find very good agreement for z_{fin} and N_{eff} both in the mass basis and in the flavor basis (with neutrino mixing). The final values of N_{eff} are 3.04483 for the case with QED corrections up to $\mathcal{O}(e^2)$ and 3.04388 for the case with those up to $\mathcal{O}(e^3)$. We also find that the difference of N_{eff} between the cases including QED corrections up to $\mathcal{O}(e^2)$ and $\mathcal{O}(e^3)$ is 0.00095, which is the same in the flavor basis. The small difference for N_{eff} in both bases may come from the fact that we neglect the off-diagonal parts for self-interaction processes in the collision terms of the Boltzmann equations.

Case	z_{fin}	N_{eff}
QED up to $\mathcal{O}(e^2)$	1.39786	3.045
QED up to $\mathcal{O}(e^3)$	1.39797	3.044

Table 3: The final values of comoving photon temperature and the effective number of neutrinos for massive neutrinos in several cases.

Case	$\delta\bar{\rho}_{\nu_1}(\%)$	$\delta\bar{\rho}_{\nu_2}(\%)$	$\delta\bar{\rho}_{\nu_3}(\%)$	$\delta\bar{n}_{\nu_1}(\%)$	$\delta\bar{n}_{\nu_2}(\%)$	$\delta\bar{n}_{\nu_3}(\%)$
QED up to $\mathcal{O}(e^2)$	0.764	0.573	0.409	0.468	0.350	0.248
QED up to $\mathcal{O}(e^3)$	0.764	0.574	0.409	0.468	0.350	0.248

Table 4: The final values of the distortions of energy densities $\delta\bar{\rho}_{\nu_i} \equiv \delta\rho_{\nu_i}/\rho_{\nu_0}$ and number densities $\delta\bar{n}_{\nu_i} \equiv (n_{\nu_i} - n_{\nu_0})/n_{\nu_0}$ for massive neutrinos in several cases.

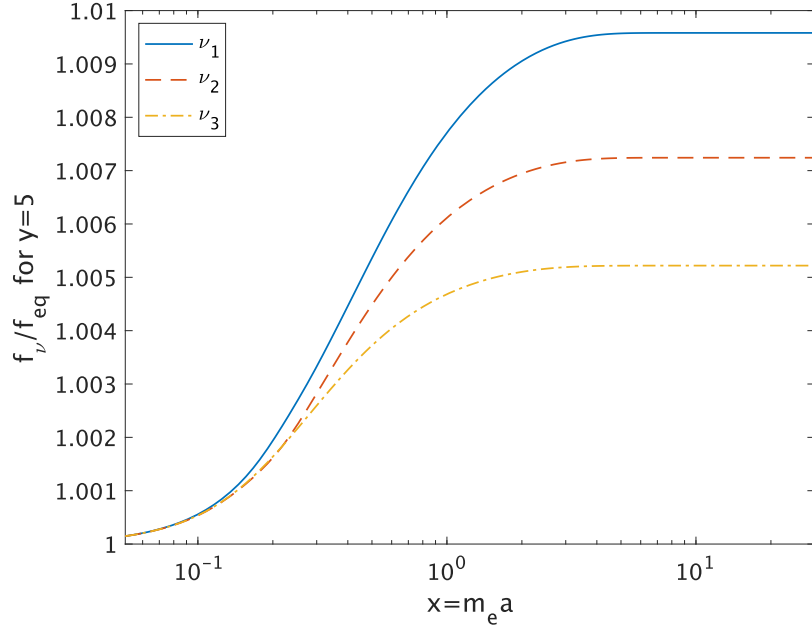


Figure 4: The time evolution of the distortions of massive neutrinos for a fixed momentum ($y = 5$) in the case with QED finite temperature corrections up to $\mathcal{O}(e^3)$.

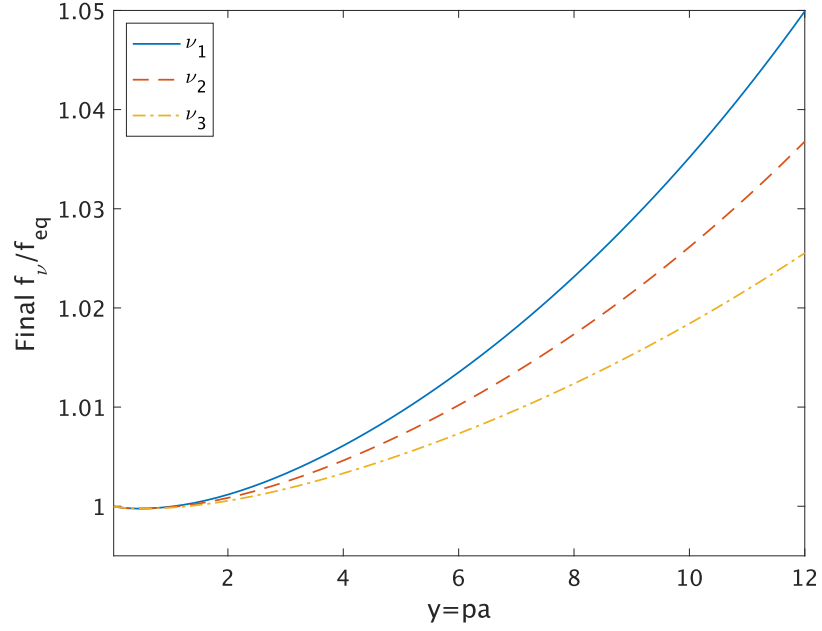


Figure 5: The final distortions of massive neutrino spectra as a function of the comoving momentum y in the case with QED finite temperature corrections up to $\mathcal{O}(e^3)$.

3.3 Transformation of distributions in the flavor and mass bases

In this section, we derive the relation between the distribution functions in the flavor and mass bases in ultra-relativistic limit and check the numerical results given in previous sections. The relation of annihilation operators for negative-helicity neutrinos between flavor and mass eigenstates is given by,

$$a_\alpha(\mathbf{p}, t) = \sum_{i=1,2,3} U_{\alpha i} a_i(\mathbf{p}, t), \quad (56)$$

with $\alpha = e, \mu, \tau$. Using the above relation, we describe the density operators for flavor neutrinos $a_\beta^\dagger a_\alpha$ through the operators for massive neutrinos,

$$a_\beta^\dagger(\mathbf{p}, t) a_\alpha(\mathbf{p}', t) = \sum_{i,j=1,2,3} U_{\beta j}^* U_{\alpha i} a_j^\dagger(\mathbf{p}, t) a_i(\mathbf{p}', t), \quad (57)$$

and we get the distribution functions for flavor neutrinos as the density matrix for massive neutrinos easily,

$$f_{\nu_\alpha}(\mathbf{p}, t) = \sum_{i,j=1,2,3} U_{\alpha j}^* U_{\alpha i} (\rho_p)_{ij}. \quad (58)$$

In particular, after the decoupling process of neutrinos, the off-diagonal parts of neutrino density matrix in the mass basis are expected to vanish since all interactions involving neutrinos are ineffective in this period and neutrinos in the mass basis do not oscillate. Then the relation between distribution functions in the flavor and mass bases after the decoupling of neutrinos is given by,

$$f_{\nu_\alpha}(\mathbf{p}, t) = \sum_i |U_{\alpha i}|^2 f_{\nu_i}(\mathbf{p}, t). \quad (59)$$

We have numerically confirmed Eq.(59) and $(\rho_p(t))_{ij} \simeq 0$ ($i \neq j$) after the decoupling of neutrinos.

4 Conclusions

We have studied the neutrino decoupling process in the early Universe by solving the kinetic equations for neutrinos numerically. We have calculated the evolution of the neutrino spectral distortions not only in the flavor basis but also in the mass basis. The latter approach enables us to easily reveal the neutrino momentum spectra at the current Universe in future work. The calculations in both bases are also useful for the cross-check of the results. In addition, in preparation for precision measurements of the effective number of neutrinos N_{eff} , we have also considered the effects due to QED finite temperature corrections up to $\mathcal{O}(e^3)$ on the relevant kinetic equations for the first time.

In both bases, we have solved the momentum-dependent kinetic equations for the neutrino density matrix, where we have considered the full collision terms for the processes

including neutrinos, electrons and their anti-particles while we neglect the off-diagonal parts of the collision terms for neutrino self-interaction processes. We find in both bases that the effective number of neutrinos is $N_{\text{eff}} = 3.044$. The effects of neutrino oscillations increase N_{eff} by about 0.0005 compared to N_{eff} without neutrino oscillations since neutrino oscillations promote the annihilation of electron-positron pairs into neutrinos. On the other hand, the impacts of QED corrections up to $\mathcal{O}(e^3)$ decrease N_{eff} by about 0.001 compared to N_{eff} with QED corrections up to $\mathcal{O}(e^2)$. We also find the final values of the number density and energy density for each neutrino. In particular, these values in the mass basis may be important for detection processes of relic neutrinos in the current Universe.

The current constraint on N_{eff} from the Planck data analyses [31] in Λ CDM model is $N_{\text{eff}} = 2.99^{+0.34}_{-0.33}$ at 95% CL [32], consistent with our prediction, $N_{\text{eff}} = 3.044$. Upcoming CMB and LSS experiments are expected to improve neutrino masses and energy density bounds over the next years (see e.g. [33, 34]) and determine N_{eff} with 1% precision in the near future (see e.g. [35–39]).

Finally, in ultra-relativistic limit and after the decoupling for neutrinos, we also find the simple transformation formula between the distribution functions in the flavor and mass bases, which is confirmed by our numerical calculation. Using this relation, we can easily switch the distribution functions in the flavor and mass bases for neutrinos without direct numerical calculations in the two bases.

Acknowledgments

We are grateful to Shoichi Yamada for useful discussions. KA is supported by JSPS Grant-in-Aid for Research Fellows No. 19J14449. KA and MY are supported in part by JSPS Bilateral Open Partnership Joint Research Projects. MY is supported in part by JSPS Grant-in-Aid for Scientific Research Numbers 18K18764 and Mitsubishi Foundation.

A Kinetic equations for neutrinos in comoving variables

In this appendix, we write the Boltzmann equations and the energy conservation law in terms of the comoving variables, $x = m_e a$, $y = pa$, $z = T_\gamma a$. In terms of these variables, we can write the Boltzmann equations (6) as in [17],

$$\frac{d\rho_y(x)}{dx} = m_{Pl} \sqrt{\frac{3}{8\pi\bar{\rho}}} \left\{ -i \frac{x^2}{m_e^3} \left[\left(\frac{M^2}{2y} - \frac{8\sqrt{2}G_F y m_e^6}{3m_W^2 x^6} \bar{E} \right), \rho_y(x) \right] + \frac{m_e^3}{x^4} \bar{C}[\rho_y(x)] \right\}. \quad (60)$$

where $\bar{\rho}$, \bar{E} , and $\bar{C}[\rho_y(x)]$ are quantities written in the comoving variables, x , y , z . We can write $\bar{\rho}$ and \bar{E} as

$$\begin{aligned}\bar{\rho} &= \rho \left(\frac{x}{m_e} \right)^4, \\ \bar{E} &= \text{diag} \left(\rho_{ee} \left(\frac{x}{m_e} \right)^4, 0, 0 \right).\end{aligned}\quad (61)$$

We also give the diagonal collision term from the self-interaction processes in the comoving variables $\bar{C}_S[\nu_\alpha(y_1)]$, where nine-dimensional collision integrals are reduced to two-dimensional collision integrals as in appendix B,

$$\begin{aligned}\bar{C}_S[\nu_\alpha(y_1)] &= \frac{G_F^2}{2\pi^3 y_1} \int dy_2 dy_3 y_2 y_3 y_4 \left[\Pi_S^1 F(\nu_\alpha^{(1)}, \nu_\alpha^{(2)}, \nu_\alpha^{(3)}, \nu_\alpha^{(4)}) \right. \\ &\quad + \Pi_S^2 F(\nu_\alpha^{(1)}, \nu_\beta^{(2)}, \nu_\alpha^{(3)}, \nu_\beta^{(4)}) + \Pi_S^3 F(\nu_\alpha^{(1)}, \nu_\alpha^{(2)}, \nu_\beta^{(3)}, \nu_\beta^{(4)}) \\ &\quad \left. + \Pi_S^2 F(\nu_\alpha^{(1)}, \nu_\gamma^{(2)}, \nu_\alpha^{(3)}, \nu_\gamma^{(4)}) + \Pi_S^3 F(\nu_\alpha^{(1)}, \nu_\alpha^{(2)}, \nu_\gamma^{(3)}, \nu_\gamma^{(4)}) \right].\end{aligned}\quad (62)$$

Similarly, the collision terms from the annihilation processes and scattering processes are

$$\begin{aligned}\bar{C}_A &= \frac{G_F^2}{2\pi^3 y_1} \int dy_2 dy_3 y_2 y_3 \bar{E}_4 \\ &\quad \times \left[\Pi_A^1 F_A^{LL}(\nu^{(1)}, \bar{\nu}^{(2)}, e^{(3)}, \bar{e}^{(4)}) + \Pi_A^2 F_A^{RR}(\nu^{(1)}, \bar{\nu}^{(2)}, e^{(3)}, \bar{e}^{(4)}) \right. \\ &\quad \left. + \Pi_A^3 \left(F_A^{RL}(\nu^{(1)}, \bar{\nu}^{(2)}, e^{(3)}, \bar{e}^{(4)}) + F_A^{LR}(\nu^{(1)}, \bar{\nu}^{(2)}, e^{(3)}, \bar{e}^{(4)}) \right) \right],\end{aligned}\quad (63)$$

$$\begin{aligned}\bar{C}_{SC} &= \frac{G_F^2}{2\pi^3 y_1} \int dy_2 dy_3 y_2 y_3 \bar{E}_4 \\ &\quad \times \left[\Pi_{SC}^1 \left(F_{SC}^{LL}(\nu^{(1)}, e^{(2)}, \nu^{(3)}, e^{(4)}) + F_{SC}^{RR}(\nu^{(1)}, e^{(2)}, \nu^{(3)}, e^{(4)}) \right) \right. \\ &\quad \left. - \Pi_{SC}^2 \left(F_{SC}^{LR}(\nu^{(1)}, e^{(2)}, \nu^{(3)}, e^{(4)}) + F_{SC}^{RL}(\nu^{(1)}, e^{(2)}, \nu^{(3)}, e^{(4)}) \right) \right],\end{aligned}\quad (64)$$

where $E_i = \sqrt{y_i^2 + x^2 + \delta\bar{m}_e^2}$ and $\delta\bar{m}_e$ is the finite temperature correction to the electron mass up to $\mathcal{O}(e^2)$ in the comoving variables,

$$\delta\bar{m}_e^2 = \frac{2\pi\alpha z}{3} + \frac{4\alpha}{\pi} \int dy \frac{y^2}{\sqrt{y^2 + x^2}} \frac{1}{\exp(\sqrt{y^2 + x^2}/z) + 1}.\quad (65)$$

The functions $\Pi_{S,A,SC}^{1,2,3}$ in Eqs. (62), (63) and (64) take the following forms,

$$\begin{aligned}
\Pi_S^1 &= 6D_1 - \frac{4D_2(y_1, y_4)}{y_1 y_4} - \frac{4D_2(y_2, y_3)}{y_2 y_3} + \frac{2D_2(y_1, y_2)}{y_1 y_2} + \frac{2D_2(y_3, y_4)}{y_3 y_4} + \frac{6D_3}{y_1 y_2 y_3 y_4}, \\
\Pi_S^2 &= 2D_1 + \frac{D_2(y_1, y_2)}{y_1 y_2} + \frac{D_2(y_3, y_4)}{y_3 y_4} - \frac{D_2(y_1, y_4)}{y_1 y_4} - \frac{D_2(y_2, y_3)}{y_2 y_3} + \frac{2D_3}{y_1 y_2 y_3 y_4}, \\
\Pi_S^3 &= D_1 - \frac{D_2(y_2, y_3)}{y_2 y_3} - \frac{D_2(y_1, y_4)}{y_1 y_4} + \frac{D_3}{y_1 y_2 y_3 y_4}, \\
\Pi_A^1 &= 2D_1 - \frac{2D_2(y_2, y_3)}{y_2 \bar{E}_3} - \frac{2D_2(y_1, y_4)}{y_1 \bar{E}_4} + \frac{2D_3}{y_1 y_2 \bar{E}_3 \bar{E}_4}, \\
\Pi_A^2 &= 2D_1 - \frac{2D_2(y_2, y_4)}{y_2 \bar{E}_4} - \frac{2D_2(y_1, y_3)}{y_1 \bar{E}_3} + \frac{D_3}{y_1 y_2 \bar{E}_3 \bar{E}_4}, \\
\Pi_A^3 &= (x^2 + \delta \bar{m}_e^2) \left(D_1 + \frac{D_2(y_1, y_2)}{y_1 y_2} \right) \frac{1}{\bar{E}_3 \bar{E}_4}, \\
\Pi_{SC}^1 &= 4D_1 - \frac{2D_2(y_2, y_3)}{\bar{E}_2 y_3} - \frac{2D_2(y_1, y_4)}{y_1 \bar{E}_4} + \frac{2D_2(y_3, y_4)}{y_3 \bar{E}_4} + \frac{2D_2(y_1, y_2)}{y_1 \bar{E}_2} + \frac{4D_3}{y_1 \bar{E}_2 y_3 \bar{E}_4}, \\
\Pi_{SC}^2 &= 2(x^2 + \delta \bar{m}_e^2) \left(D_1 - \frac{D_2(y_1, y_3)}{y_1 y_3} \right) \frac{1}{\bar{E}_2 \bar{E}_4}.
\end{aligned} \tag{66}$$

The functions of $D_{1,2,3}$ are written as,

$$\begin{aligned}
D_1 &= \frac{4}{\pi} \int_0^\infty \frac{d\lambda}{\lambda^2} \sin(\lambda y_1) \sin(\lambda y_2) \sin(\lambda y_3) \sin(\lambda y_4), \\
D_2(y_3, y_4) &= \frac{4y_3 y_4}{\pi} \int_0^\infty \frac{d\lambda}{\lambda^2} \sin(\lambda y_1) \sin(\lambda y_2) \left[\cos(\lambda y_3) - \frac{\sin(\lambda y_3)}{\lambda y_3} \right] \left[\cos(\lambda y_4) - \frac{\sin(\lambda y_4)}{\lambda y_4} \right], \\
D_3 &= \frac{4y_1 y_2 y_3 y_4}{\pi} \int_0^\infty \frac{d\lambda}{\lambda^2} \left[\cos(\lambda y_1) - \frac{\sin(\lambda y_1)}{\lambda y_1} \right] \left[\cos(\lambda y_2) - \frac{\sin(\lambda y_2)}{\lambda y_2} \right] \\
&\quad \times \left[\cos(\lambda y_3) - \frac{\sin(\lambda y_3)}{\lambda y_3} \right] \left[\cos(\lambda y_4) - \frac{\sin(\lambda y_4)}{\lambda y_4} \right],
\end{aligned} \tag{67}$$

which can be integrated analytically as in appendix B.

Finally, the energy conservation law (20) is translated into the evolution equation for z , including the finite temperature corrections from QED up to $\mathcal{O}(e^3)$ [11, 28],

$$\frac{dz}{dx} = \frac{\frac{x}{z} J(x/z) - \frac{1}{2\pi^2 z^3} \int_0^\infty dy y^3 \left(\frac{df_{\nu_e}}{dx} + \frac{df_{\nu_\mu}}{dx} + \frac{df_{\nu_\tau}}{dx} \right) + G_1^{(2)}(x/z) + G_1^{(3)}(x/z)}{\frac{x^2}{z^2} J(x/z) + Y(x/z) + \frac{2\pi^2}{15} + G_2^{(2)}(x/z) + G_2^{(3)}(x/z)}, \tag{68}$$

where

$$\begin{aligned}
G_1^{(2)}(\omega) &= 2\pi\alpha \left[\frac{1}{\omega} \left(\frac{K(\omega)}{3} + 2K(\omega)^2 - \frac{J(\omega)}{6} - K(\omega)J(\omega) \right) \right. \\
&\quad \left. + \left(\frac{K'(\omega)}{6} - K(\omega)K'(\omega) + \frac{J'(\omega)}{6} + J'(\omega)K(\omega) + J(\omega)K'(\omega) \right) \right], \\
G_2^{(2)}(\omega) &= -8\pi\alpha \left(\frac{K(\omega)}{6} + \frac{J(\omega)}{6} - \frac{1}{2}K(\omega)^2 + K(\omega)J(\omega) \right) \\
&\quad + 2\pi\alpha\omega \left(\frac{K'(\omega)}{6} - K(\omega)K'(\omega) + \frac{J'(\omega)}{6} + J'(\omega)K(\omega) + J(\omega)K'(\omega) \right) \\
G_1^{(3)}(\omega) &= \frac{e^3}{4\pi} \left(K(\omega) + \frac{\omega^2}{2}k(\omega) \right)^{1/2} \left[\frac{1}{\omega} (2J(\omega) - 4K(\omega)) - 2J'(\omega) - \omega^2 j'(\omega) \right. \\
&\quad \left. - \omega (2k(\omega) + j(\omega)) - \frac{(2J(\omega) + \omega^2 j(\omega)) (\omega (k(\omega) - j(\omega)) + K'(\omega))}{2(2K + \omega^2 k(\omega))} \right] \\
G_2^{(3)}(\omega) &= \frac{e^3}{4\pi} \left(K(\omega) + \frac{\omega^2}{2}k(\omega) \right)^{1/2} \left[\frac{(2J(\omega) + \omega^2 j(\omega))^2}{2(2K(\omega) + \omega^2 k(\omega))} - \frac{2}{\omega} Y'(\omega) - \omega (3J'(\omega) + \omega^2 j'(\omega)) \right]
\end{aligned} \tag{69}$$

with

$$\begin{aligned}
K(\omega) &= \frac{1}{\pi^2} \int_0^\infty du \frac{u^2}{\sqrt{u^2 + \omega^2}} \frac{1}{\exp(\sqrt{u^2 + \omega^2}) + 1}, \\
J(\omega) &= \frac{1}{\pi^2} \int_0^\infty du u^2 \frac{\exp(\sqrt{u^2 + \omega^2})}{(\exp(\sqrt{u^2 + \omega^2}) + 1)^2}, \\
Y(\omega) &= \frac{1}{\pi^2} \int_0^\infty du u^4 \frac{\exp(\sqrt{u^2 + \omega^2})}{(\exp(\sqrt{u^2 + \omega^2}) + 1)^2}, \\
k(\omega) &= \frac{1}{\pi^2} \int_0^\infty du \frac{1}{\sqrt{u^2 + \omega^2}} \frac{1}{\exp(\sqrt{u^2 + \omega^2}) + 1}, \\
j(\omega) &= \frac{1}{\pi^2} \int_0^\infty du \frac{\exp(\sqrt{u^2 + \omega^2})}{(\exp(\sqrt{u^2 + \omega^2}) + 1)^2}.
\end{aligned} \tag{70}$$

The prime represents the derivative with respect to ω . Note that $G^{(2)}$ and $G^{(3)}$ indicate the finite temperature corrections at $\mathcal{O}(e^2)$ and $\mathcal{O}(e^3)$ respectively.

B Analytic estimation of the collision integral

In this appendix, we analytically perform seven out of nine integrations in the collision terms for four-Fermi interaction processes in the isotropic Universe, following refs. [7, 23].

We consider the general form of the collision term in this case,

$$C_{\text{coll}} = \frac{1}{2E_1} \int (2\pi)^4 \delta^4(\sum_i p_i) |\mathcal{M}|^2 F(\rho_p) \prod_{i=2}^4 \frac{d^3 \mathbf{p}_i}{(2\pi)^3 2E_i}, \quad (71)$$

where E_i is the energy of i -th particle. The matrix $F(\rho_p)$ is a function of neutrino density matrix and $|\mathcal{M}|^2$ is a part of the possible squared amplitudes summed over spin degrees of freedom of all particles except for the first particle. We use the following relation:

$$\delta^{(3)}(\sum_i \mathbf{p}_i) = \int e^{\boldsymbol{\lambda} \cdot (\mathbf{p}_1 + \mathbf{p}_2 - \mathbf{p}_3 - \mathbf{p}_4)} \frac{d^3 \boldsymbol{\lambda}}{(2\pi)^3}, \quad (72)$$

and decompose momentum integrations into the radial integration and the angle integrations,

$$d^3 \mathbf{p}_i = p_i^2 dp_i \sin \theta_i d\theta_i d\phi_i \equiv p_i^2 dp_i d\Omega_i. \quad (73)$$

Using Eqs. (72) and (73), we write the general collision term (71) as

$$C_{\text{coll}} = \frac{1}{64\pi^3 E_1 p_1} \int \delta(E_1 + E_2 - E_3 - E_4) F(\rho_p(t)) D(p_1, p_2, p_3, p_4) \frac{p_2 dp_2}{E_2} \frac{p_3 dp_3}{E_3} \frac{p_4 dp_4}{E_4}, \quad (74)$$

where

$$\begin{aligned} D(p_1, p_2, p_3, p_4) &= \frac{p_1 p_2 p_3 p_4}{64\pi^5} \int_0^\infty \lambda^2 d\lambda \int e^{i\boldsymbol{\lambda} \cdot \mathbf{p}_1} d\Omega_{\boldsymbol{\lambda}} \int e^{i\boldsymbol{\lambda} \cdot \mathbf{p}_2} d\Omega_{\mathbf{p}_2} \\ &\quad \times \int e^{-i\boldsymbol{\lambda} \cdot \mathbf{p}_3} d\Omega_{\mathbf{p}_3} \int e^{-i\boldsymbol{\lambda} \cdot \mathbf{p}_4} d\Omega_{\mathbf{p}_4} |\mathcal{M}|^2. \end{aligned} \quad (75)$$

In the cases of four-Fermi interaction processes, all of $|\mathcal{M}|^2$ have two kinds of forms,

$$K_1(q_{1\mu} q_2^\mu)(q_{3\nu} q_4^\nu) = K_1(E_1 E_2 - \mathbf{q}_1 \cdot \mathbf{q}_2)(E_3 E_4 - \mathbf{q}_3 \cdot \mathbf{q}_4), \quad (76)$$

$$K_2 m^2(q_{3\mu} q_4^\mu) = K_2 m^2(E_3 E_4 - \mathbf{q}_3 \cdot \mathbf{q}_4), \quad (77)$$

where q_i corresponds to one of p_j and the angle between \mathbf{q}_i and \mathbf{q}_j is written in terms of the integration variables of angle,

$$\cos \psi_{ij} = \sin \theta_i \sin \theta_j \cos(\phi_i - \phi_j) + \cos \theta_i \cos \theta_j. \quad (78)$$

In both cases of Eqs. (76) and (77), we can perform all angle integrals in Eq. (75) so that we can write $D(q_1, q_2, q_3, q_4)$ in the case of Eq. (76) as

$$D = K_1 [E_1 E_2 E_3 E_4 D_1 + E_1 E_2 D_2(q_3, q_4) + E_3 E_4 D_2(q_1, q_2) + D_3], \quad (79)$$

while in the case of Eq. (77), $D(q_1, q_2, q_3, q_4)$ is expressed as

$$D = K_2 E_1 E_2 [E_3 E_4 D_1 + D_2(q_3, q_4)]. \quad (80)$$

Here $D_{1,2,3}$ are defined in Eq. (67) and hereafter we only consider $D_1, D_2(q_3, q_4), D_3$.

Although we can perform the integrals in $D_{1,2,3}$ and get the exact expressions given in ref. [23], we assume for simplicity that $q_1 > q_2$ and $q_3 > q_4$ without loss of generality. Then we get the simplified expressions of $D_{1,2,3}$ in four different cases:

(1) $q_1 + q_2 > q_3 + q_4$, $q_1 + q_4 > q_2 + q_3$ and $q_1 \leq q_2 + q_3 + q_4$

$$\begin{aligned} D_1 &= \frac{1}{2}(q_2 + q_3 + q_4 - q_1), \\ D_2(q_3, q_4) &= \frac{1}{12} \left((q_1 - q_2)^3 + 2(q_3^3 + q_4^3) - 3(q_1 - q_2)(q_3^2 + q_4^2) \right), \\ D_3 &= \frac{1}{60} \left(q_1^5 - 5q_1^3 q_2^2 + 5q_1^2 q_2^3 - q_2^5 \right. \\ &\quad - 5q_1^3 q_3^2 + 5q_2^3 q_3^2 + 5q_1^2 q_3^3 + 5q_2^2 q_3^3 - q_3^5 \\ &\quad \left. - 5q_1^3 q_4^2 + 5q_2^3 q_4^2 + 5q_1^2 q_4^3 + 5q_2^2 q_4^3 + 5q_3^2 q_4^3 - q_4^5 \right). \end{aligned} \quad (81)$$

Note that the case $q_1 > q_2 + q_3 + q_4$ is unphysical so that $D_1 = D_2 = D_3 = 0$ in this case.

(2) $q_1 + q_2 > q_3 + q_4$ and $q_1 + q_4 < q_2 + q_3$

$$\begin{aligned} D_1 &= q_4, \\ D_2(q_3, q_4) &= \frac{1}{3} q_4^3, \\ D_3 &= \frac{1}{30} q_4^3 (5q_1^2 + 5q_2^2 + 5q_3^2 - q_4^2). \end{aligned} \quad (82)$$

(3) $q_1 + q_2 < q_3 + q_4$, $q_1 + q_4 < q_2 + q_3$ and $q_3 \leq q_1 + q_2 + q_4$

$$\begin{aligned} D_1 &= \frac{1}{2}(q_1 + q_2 + q_4 - q_3), \\ D_2(q_3, q_4) &= \frac{1}{12} \left(-(q_1 + q_2)^3 - 2q_3^3 + 2q_4^3 + 3(q_1 + q_2)(q_3^2 + q_4^2) \right). \end{aligned} \quad (83)$$

D_3 is equal to that in Eq. (81) with the replacement of variables $q_1 \leftrightarrow q_3$ and $q_2 \leftrightarrow q_4$ and the case $q_3 > q_1 + q_2 + q_4$ is unphysical so that $D_1 = D_2 = D_3 = 0$ in this case.

(4) $q_1 + q_2 < q_3 + q_4$ and $q_1 + q_4 > q_2 + q_3$

$$\begin{aligned} D_1 &= q_2, \\ D_2(q_3, q_4) &= \frac{1}{6} q_2 (3q_3^2 + 3q_4^2 - 3q_1^2 - q_2^2), \\ D_3 &= \frac{1}{30} q_2^3 (5q_1^2 + 5q_3^2 + 5q_4^2 - q_2^2). \end{aligned} \quad (84)$$

After we have integrated the δ -function, we get the simplified expression of the collision term, leaving two integrals,

$$C_{\text{coll}} = \frac{1}{64\pi^3 E_1 p_1} \int \int F(\rho_p(t)) D(p_1, p_2, p_3, p_4) \frac{p_2 dp_2}{E_2} \frac{p_3 dp_3}{E_3}, \quad (85)$$

where $E_4 = E_1 + E_2 - E_3$ and $p_4 = \sqrt{E_4^2 - m_4^2}$.

References

- [1] D. A. Dicus, E. W. Kolb, A. M. Gleeson, E. C. G. Sudarshan, V. L. Teplitz and M. S. Turner, Phys. Rev. D **26**, 2694 (1982). doi:10.1103/PhysRevD.26.2694
- [2] A. D. Dolgov, Phys. Rept. **370**, 333 (2002) doi:10.1016/S0370-1573(02)00139-4 [hep-ph/0202122].
- [3] S. Dodelson and M. S. Turner, Phys. Rev. D **46**, 3372 (1992). doi:10.1103/PhysRevD.46.3372
- [4] A. D. Dolgov and M. Fukugita, Phys. Rev. D **46**, 5378 (1992). doi:10.1103/PhysRevD.46.5378
- [5] B. D. Fields, S. Dodelson and M. S. Turner, Phys. Rev. D **47**, 4309 (1993) doi:10.1103/PhysRevD.47.4309 [astro-ph/9210007].
- [6] S. Hannestad and J. Madsen, Phys. Rev. D **52**, 1764 (1995) doi:10.1103/PhysRevD.52.1764 [astro-ph/9506015].
- [7] A. D. Dolgov, S. H. Hansen and D. V. Semikoz, Nucl. Phys. B **503**, 426 (1997) doi:10.1016/S0550-3213(97)00479-3 [hep-ph/9703315].
- [8] A. D. Dolgov, S. H. Hansen and D. V. Semikoz, Nucl. Phys. B **543**, 269 (1999) doi:10.1016/S0550-3213(98)00818-9 [hep-ph/9805467].
- [9] S. Esposito, G. Miele, S. Pastor, M. Peloso and O. Pisanti, Nucl. Phys. B **590**, 539 (2000) doi:10.1016/S0550-3213(00)00554-X [astro-ph/0005573].
- [10] N. Fornengo, C. W. Kim and J. Song, Phys. Rev. D **56**, 5123 (1997) doi:10.1103/PhysRevD.56.5123 [hep-ph/9702324].
- [11] G. Mangano, G. Miele, S. Pastor and M. Peloso, Phys. Lett. B **534**, 8 (2002) doi:10.1016/S0370-2693(02)01622-2 [astro-ph/0111408].
- [12] J. Birrell, C. T. Yang and J. Rafelski, Nucl. Phys. B **890**, 481 (2014) doi:10.1016/j.nuclphysb.2014.11.020 [arXiv:1406.1759 [nucl-th]].
- [13] E. Grohs, G. M. Fuller, C. T. Kishimoto, M. W. Paris and A. Vlasenko, Phys. Rev. D **93**, no. 8, 083522 (2016) doi:10.1103/PhysRevD.93.083522 [arXiv:1512.02205 [astro-ph.CO]].
- [14] E. Grohs and G. M. Fuller, Nucl. Phys. B **923**, 222 (2017) doi:10.1016/j.nuclphysb.2017.07.019 [arXiv:1706.03391 [astro-ph.CO]].

- [15] J. Froustey and C. Pitrou, Phys. Rev. D **101**, no. 4, 043524 (2020) doi:10.1103/PhysRevD.101.043524 [arXiv:1912.09378 [astro-ph.CO]].
- [16] G. Mangano, G. Miele, S. Pastor, T. Pinto, O. Pisanti and P. D. Serpico, Nucl. Phys. B **729**, 221 (2005) doi:10.1016/j.nuclphysb.2005.09.041 [hep-ph/0506164].
- [17] P. F. de Salas and S. Pastor, JCAP **1607**, 051 (2016) doi:10.1088/1475-7516/2016/07/051 [arXiv:1606.06986 [hep-ph]].
- [18] S. Gariazzo, P. F. de Salas and S. Pastor, JCAP **1907**, 014 (2019) doi:10.1088/1475-7516/2019/07/014 [arXiv:1905.11290 [astro-ph.CO]].
- [19] A. D. Dolgov, S. H. Hansen, S. Pastor, S. T. Petcov, G. G. Raffelt and D. V. Semikoz, Nucl. Phys. B **632**, 363 (2002) doi:10.1016/S0550-3213(02)00274-2 [hep-ph/0201287].
- [20] G. Mangano, G. Miele, S. Pastor, O. Pisanti and S. Sarikas, Phys. Lett. B **708**, 1 (2012) doi:10.1016/j.physletb.2012.01.015 [arXiv:1110.4335 [hep-ph]].
- [21] E. Castorina, U. Franca, M. Lattanzi, J. Lesgourgues, G. Mangano, A. Melchiorri and S. Pastor, Phys. Rev. D **86**, 023517 (2012) doi:10.1103/PhysRevD.86.023517 [arXiv:1204.2510 [astro-ph.CO]].
- [22] G. Sigl and G. Raffelt, Nucl. Phys. B **406**, 423 (1993). doi:10.1016/0550-3213(93)90175-O
- [23] D. N. Blaschke and V. Cirigliano, Phys. Rev. D **94**, no. 3, 033009 (2016) doi:10.1103/PhysRevD.94.033009 [arXiv:1605.09383 [hep-ph]].
- [24] D. Notzold and G. Raffelt, Nucl. Phys. B **307**, 924-936 (1988) doi:10.1016/0550-3213(88)90113-7
- [25] I. Esteban, M. C. Gonzalez-Garcia, A. Hernandez-Cabezudo, M. Maltoni and T. Schwetz, JHEP **1901**, 106 (2019) doi:10.1007/JHEP01(2019)106 [arXiv:1811.05487 [hep-ph]].
- [26] A. F. Heckler, Phys. Rev. D **49**, 611 (1994). doi:10.1103/PhysRevD.49.611
- [27] R. E. Lopez and M. S. Turner, Phys. Rev. D **59**, 103502 (1999) doi:10.1103/PhysRevD.59.103502 [astro-ph/9807279].
- [28] J. J. Bennett, G. Buldgen, M. Drewes and Y. Y. Y. Wong, JCAP **2003**, no. 03, 003 (2020) doi:10.1088/1475-7516/2020/03/003 [arXiv:1911.04504 [hep-ph]].
- [29] S. Hannestad, Phys. Rev. D **65**, 083006 (2002) doi:10.1103/PhysRevD.65.083006 [astro-ph/0111423].
- [30] M. Escudero Abenza, arXiv:2001.04466 [hep-ph].
- [31] Y. Akrami *et al.* [Planck], [arXiv:1807.06205 [astro-ph.CO]].

- [32] N. Aghanim *et al.* [Planck], [arXiv:1807.06209 [astro-ph.CO]].
- [33] B. Benson *et al.* [SPT-3G], Proc. SPIE Int. Soc. Opt. Eng. **9153**, 91531P (2014) doi:10.1117/12.2057305 [arXiv:1407.2973 [astro-ph.IM]].
- [34] P. Ade *et al.* [Simons Observatory], JCAP **02**, 056 (2019) doi:10.1088/1475-7516/2019/02/056 [arXiv:1808.07445 [astro-ph.CO]].
- [35] K. Abazajian *et al.* [Topical Conveners: K.N. Abazajian, J.E. Carlstrom, A.T. Lee], Astropart. Phys. **63**, 66-80 (2015) doi:10.1016/j.astropartphys.2014.05.014 [arXiv:1309.5383 [astro-ph.CO]].
- [36] E. Di Valentino *et al.* [CORE], JCAP **04**, 017 (2018) doi:10.1088/1475-7516/2018/04/017 [arXiv:1612.00021 [astro-ph.CO]].
- [37] S. Hanany *et al.* [NASA PICO], [arXiv:1902.10541 [astro-ph.IM]].
- [38] N. Sehgal *et al.* [arXiv:1906.10134 [astro-ph.CO]].
- [39] K. Abazajian *et al.* [arXiv:1907.04473 [astro-ph.IM]].